Co-design of output feedback laws and event-triggering conditions for the L2 -stabilization of linear systems

Mahmoud Abdelrahim, Romain Postoyan, Jamal Daafouz, Dragan Nešić, Maurice Heemels

Co-design of output feedback laws and event-triggering conditions for the $\mathcal{L}_2$-stabilization of linear systems

M. Abdelrahim[a,e], R. Postoyan[b,c], J. Daafouz[b,c], D. Nešić[d], W.P.M.H. Heemels[a]

[a] *Department of Mechanical Engineering, Eindhoven University of Technology, The Netherlands*
[b] *Université de Lorraine, CRAN, UMR 7039, France*
[c] *CNRS, CRAN, UMR 7039, France*
[d] *Department of Electrical and Electronic Engineering and MIDAS Laboratory, the University of Melbourne, Australia*
[e] *Department of Mechanical Engineering, Assiut University, Egypt*

Abstract

We investigate the $\mathcal{L}_2$-stabilization of linear systems using output feedback event-triggered controllers. In particular, we are interested in the scenario where the plant output and the control input are transmitted to the controller and to the actuators, respectively, over two different digital channels, which have their own sampling rule. The plant dynamics is affected by external disturbances and the output measurement and the control input are corrupted by noises. We present a co-design procedure to simultaneously synthesize dynamic output feedback laws and event-triggering conditions such that the closed-loop system is $\mathcal{L}_2$-stable with a given upper-bound on the $\mathcal{L}_2$-gain. The required conditions are formulated in terms of the feasibility of linear matrix inequalities (LMIs). Then, we exploit these LMIs to maximize the guaranteed minimum time between two transmissions of the plant output and/or of the control input. We also present a heuristic method to reduce the amount of transmissions for each channel. The developed technique encompasses time-driven (and so periodic) sampling as a particular case and the result is also new in this context. The effectiveness of the proposed methods is illustrated on a numerical example.

1 Introduction

In event-triggered control, the feedback loop is closed only when a state/output dependent criterion is violated. As a result, the amount of communication between the sensors, the controllers, and the actuators is adapted to the current state of the controlled system, which may be significantly reduced compared to conventional time-triggered setups, see [12] and the references therein. This feature is particularly appealing when the communication resources are limited and need to be efficiently used such as in networked control systems (NCS), in which the feedback information and the control input updates are transmitted over a shared network.

Most existing event-triggering strategies are developed using the emulation approach, see, e.g., [21] and the references therein. In other words, the feedback law is first synthesized to stabilize the plant in the absence of network. Afterwards, the effect of network is considered and the sampling rule is constructed. A possible disadvantage of emulation is that the performance of the system, like the (guaranteed) $\mathcal{L}_2$-gain, is limited by the initial choice of the feedback law. To overcome this restriction, the controller and the event-triggering condition should be designed simultaneously, which is usually more challenging. In this respect, three directions of research are proposed in the literature: the joint design of control inputs and self-triggering conditions, e.g., [11, 14], optimal event-triggered control, e.g., [3, 17], and the co-design of feedback laws and event-triggering conditions, e.g., [6,15,16,25]. We are interested in the last approach.

We consider the scenario where the plant dynamics is linear time-invariant (LTI) and is affected by external disturbances and both the output measurement and the control input are corrupted by noises. We assume that the plant output and the control input are transmitted over two different channels, which are governed by two

⋆ M. Abdelrahim and W.P.M.H. Heemels are supported by the Dutch Science Foundation (STW) and the Dutch Organization for Scientific Research (NWO) under the VICI grant "Wireless control systems: A new frontier in automation" (No. 11382). R. Postoyan and J. Daafouz are partially supported by the ANR under the grant COMPACS (ANR-13-BS03-0004-02). D. Nešić work is supported by the Australian Research Council under the Discovery Projects scheme.

Email addresses: m.abdelrahim@aun.edu.eg (M. Abdelrahim), romain.postoyan@univ-lorraine.fr (R. Postoyan), jamal.daafouz@univ-lorraine.fr (J. Daafouz), dnesic@unimelb.edu.au (D. Nešić), m.heemels@tue.nl (W.P.M.H. Heemels).

independent event-triggering conditions. Each triggering condition can only depend on the information available locally at each channel, that is the noisy measurement of the plant output or of the noisy control input. Similar setups have been studied in [2, 8] but with the emulation approach. Our objective here is to co-design dynamic output feedback laws and the triggering rules to ensure the $\mathcal{L}_2$-stability of the closed-loop system with a given upper-bound on the $\mathcal{L}_2$-gain.

We consider dynamic output feedback laws of the same dimension as the plant, as well as the same type of triggering rules as in [2]. The difference is that we want to design both the controller and the parameters of the triggering rules simultaneously. The triggering rules consist in waiting fixed amount of times $T_y, T_u > 0$ since the last transmission instant of the plant output and of the control input, respectively, and then checking the event-triggering rules. The enforced bounds T_y and T_u exclude the occurrence of Zeno behaviour at each channel, which might appear otherwise. The overall system is modeled as a hybrid system in the formalism of [10]. We first revisit the results presented in [2] for LTI systems to ease the development of a co-design procedure afterwards. In particular, we provide a new linear matrix inequality (LMI), which ensures the $\mathcal{L}_2$-stability of the closed-loop system, by making different modeling and design choices. Still, this matrix inequality becomes nonlinear when the feedback law has to be designed and standard linearization techniques, like congruence transformations cannot be applied. To overcome this issue, we introduce additional LMI constraints. The LMI formulation of the co-design algorithm is then exploited to adapt some transmission characteristics given a desired bound on the $\mathcal{L}_2$-gain, which quantifies the robustness of the system. First, the LMI conditions are exploited to maximize the guaranteed minimum times T_y, T_u. This task is motivated by the fact that the resulting T_y, T_u may be very small, and thus may not meet the hardware limitations because of the choice of the feedback law. Hence, it is of interest to enlarge the lower bounds T_y, T_u, which are the true minimum times between two successive transmissions on the corresponding channel, as we will prove. Second, we present a heuristic method to enlarge the inter-transmission times of the output measurement and of the control input, which may lead to further reductions in the amount of transmissions. The effectiveness of the approach is illustrated on a numerical example. The simulations show that the co-design technique leads to a great reduction in the amount of transmissions compared to the emulation approach while guaranteeing the same (or slightly increased) estimate of the $\mathcal{L}_2$-gain. The results also encompass the particular case of time-triggered control as the guaranteed minimum times T_y, T_u mentioned above can be used as a maximum sampling period for each corresponding channel.

Compared to [6, 15, 16, 25], we synthesize *continuous* event-triggered controllers while these works are all dedicated to the case of *discrete* event-triggered control, i.e., the plant dynamics is first discretized and then an event-triggered controller is designed for the discrete-time system, which is a different sampling paradigm. Moreover, we consider different types of exogenous inputs affecting the control system, as the plant is subject to external disturbances and both the output measurement and the control input are corrupted by noise. The effect of noise on the transmitted variables is not trivial to handle and has only been considered in [6] for the plant output only, but not for the control input. Furthermore, we give analytical insights on the potential of the co-design technique to generate less transmissions than with the emulation approach, which has not been studied before in the literature, to the best of our knowledge.

Compared to the preliminary version of this work [1], we investigate robust stabilization, namely $\mathcal{L}_2$-stability, as opposed to asymptotic stabilization. Moreover, inspired by [2,8], the proposed technique applies to the case where the plant output and the control input are transmitted asynchronously, which is different than the setup studied in [1], where both transmissions occur synchronously.

The rest of the paper is organized as follows. Preliminaries are given in Section 2. The hybrid model and the problem formulation are presented in Section 3. We first design event-triggered controllers by emulation in Section 4. Then, the co-design procedure is developed in Section 5. We discuss how to optimize the parameters of the event-triggering mechanism in Section 6. Numerical simulations are given in Section 7. Conclusions are provided in Section 8. The proofs are given in the Appendix.

2 Preliminaries

Let $\mathbb{R} := (-\infty, \infty)$, $\mathbb{R}_{\geq 0} := [0, \infty)$, $\mathbb{Z}_{\geq 0} := \{0, 1, 2, \ldots\}$ and $\mathbb{Z}_{>0} := \{1, 2, \ldots\}$. A continuous function $\gamma : \mathbb{R}_{\geq 0} \to \mathbb{R}_{\geq 0}$ is of class $\mathcal{K}$ if it is zero at zero, strictly increasing, and it is of class $\mathcal{K}_\infty$ if in addition $\gamma(s) \to \infty$ as $s \to \infty$. We write A^T and A^{-T} to respectively denote the transpose and the inverse of transpose of A (when it exists) and $\operatorname{diag}(A_1, \cdots, A_N)$ is the block-diagonal matrix with the entries $A_1, \cdots, A_N$ on the diagonal. The symbol $\star$ stands for symmetric blocks in matrices. We use $\mathbb{I}_n$ to denote the identity matrix of dimension n. We denote by $|.|$ the Euclidean norm. We use (x, y) to represent the vector $[x^T, y^T]^T$ for $x \in \mathbb{R}^n$ and $y \in \mathbb{R}^m$.

The Schur complement formula states that an LMI $\left[\begin{smallmatrix} A & B^T \\ B & C \end{smallmatrix}\right] < 0$ is satisfied when $C < 0$ and $A - B^T C^{-1} B < 0$ both hold.

We consider hybrid systems of the following form [4, 10]

$$\dot{x} = F(x, w) \quad x \in \mathcal{C}, \quad x^+ \in G(x) \quad x \in \mathcal{D}, \qquad (1)$$

where $x \in \mathbb{R}^{n_x}$ is the state, $w \in \mathbb{R}^{n_w}$ is an exogenous input, $\mathcal{C}$ is the flow set, F is the flow map, $\mathcal{D}$ is the jump set and G is the jump map. The exogenous input w only affects the flow dynamics in (1) and not the flow and the jump sets, as this will be the case in this study. For more details on the notion of solution for system (1), we refer the reader to [4, 10].

We adopt the following definition of $\mathcal{L}_2$-norm of hybrid signals [20].

Definition 1 *For a hybrid signal z defined on the hybrid time domain* $\operatorname{dom} z = \bigcup_{j=0}^{J-1} [t_j, t_{j+1}] \times \{j\}$ *with J possibly ∞ and/or $t_J = \infty$, the $\mathcal{L}_2$-norm of z is defined as* $||z||_2 := \left(\sum_{j=0}^{J-1} \int_{t_j}^{t_{j+1}} |z(t,j)|^2 dt \right)^{\frac{1}{2}}$*, provided that the right-hand side exists and is finite, in which case we write $z \in \mathcal{L}_2$.* □

Based on Definition 1, we define $\mathcal{L}_2$-stability for system (1) as in [13, 20].

Definition 2 *System (1) is $\mathcal{L}_2$-stable from the input $w \in \mathcal{L}_2$ to the output $z := h(x, w)$ with gain less than or equal to $\eta \geq 0$ if there exists $\beta \in \mathcal{K}_\infty$ such that any solution pair (x, w) to (1) satisfies $||z||_2 \leq \beta(|x(0,0)|) + \eta ||w||_2$.* □

3 Hybrid model and problem statement

Consider the LTI plant model

$$\dot{x}_p = A_p x_p + B_p \hat{u} + E_p w, \quad y = C_p x_p + d_y, \tag{2}$$

where $x_p \in \mathbb{R}^{n_p}$ is the plant state, $\hat{u} \in \mathbb{R}^{n_u}$ is the most recently transmitted value of the control input $u \in \mathbb{R}^{n_u}$ to the plant, $w \in \mathbb{R}^{n_w}$ is an external disturbance on the plant, $y \in \mathbb{R}^{n_y}$ is the measured output, which is affected by the additive measurement noise $d_y \in \mathbb{R}^{n_y}$. We assume that $w \in \mathcal{L}_2$, and that the signal d_y is absolutely continuous and its time-derivative exists for almost all the time and is in $\mathcal{L}_2$. We focus on dynamic controllers of the form

$$\dot{x}_c = A_c x_c + B_c \hat{y}, \quad u = C_c x_c + d_u, \tag{3}$$

where $x_c \in \mathbb{R}^{n_c}$ is the controller state, $\hat{y} \in \mathbb{R}^{n_y}$ is the most recently transmitted value of the output measurement y to the controller, and $d_u \in \mathbb{R}^{n_u}$ is a vector of noises affecting the control input, e.g., additive torque disturbance in robotic systems [7] or acceleration disturbances on the control input in the vertical takeoff and landing (VTOL) aircraft [5]. We assume that the signal d_u is absolutely continuous and its time-derivative exists for almost all the time and is in $\mathcal{L}_2$. We consider that $n_c = n_p$, i.e., the plant state and the controller state are of the same dimension.

We study the scenario where the communications between plant (2) and controller (3) are realized over digital channels, see Figure 1. In particular, the transmission instants $t_i^y, i \in \mathcal{I}_y \subseteq \mathbb{Z}_{\geq 0}$ of the output measurement and the update instants $t_i^u, i \in \mathcal{I}_u \subseteq \mathbb{Z}_{\geq 0}$ of the control input are generated by two independent triggering conditions. Hence, $t_i^y \neq t_j^u, i = j$ in general, i.e., t_i^y and t_j^u are not necessarily synchronized a priori, see also [8, 9].

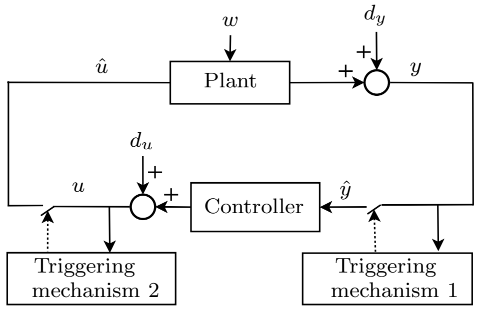

Fig. 1. Asynchronous event-triggered control.

At each transmission instant $t_i^y, i \in \mathcal{I}_y$, the current output measurement y is transmitted to the controller to update the value of $\hat{y}$ in (3). On the other hand, the control input u is only broadcasted to the actuators at transmission instants $t_i^u, i \in \mathcal{I}_u$ to update $\hat{u}$ in (2). We ignore possible transmissions delays, but these can be handled as in [23]. The values of $\hat{y}$ and $\hat{u}$ are kept constant between two successive transmission instants of the output measurement and of the control input, respectively, by means of zero-order-hold elements. At each transmission instant t_i^y, $\hat{y}$ is reset to the actual value of y. Similarly, $\hat{u}$ is reset to the actual value of u at t_j^u. We define the network-induced error as $e_y = \hat{y} - y$ and $e_u = \hat{u} - u$. Hence, e_y and e_u are reset to zero at $t_i^y, i \in \mathcal{I}_y$ and at $t_j^u, j \in \mathcal{I}_u$, respectively.

We introduce two timers $\tau_y, \tau_u \in \mathbb{R}_{\geq 0}$ to describe the time elapsed since the last transmission instant of y and of u, respectively, which have the dynamics

$$\begin{array}{ll} \dot{\tau}_y = 1 \text{ for almost all } t \in [t_i^y, t_{i+1}^y], & \tau_y(t_i^{y+}) = 0 \\ \dot{\tau}_u = 1 \text{ for almost all } t \in [t_i^u, t_{i+1}^u], & \tau_u(t_i^{u+}) = 0. \end{array} \tag{4}$$

These variables will be useful to define the triggering conditions.

Define $C_y := \begin{bmatrix} C_p & 0 \end{bmatrix}$, $C_u := \begin{bmatrix} 0 & C_c \end{bmatrix}$ and let $x := (x_p, x_c) \in \mathbb{R}^{n_p + n_c}$, $q := (x, e_y, e_u, \tau_y, \tau_u) \in \mathbb{R}^{n_q}$ with $n_q = \mathbb{R}^{n_p + n_c + n_y + n_u + 2}$, $\xi := (w, d_y, d_u) \in \mathbb{R}^{n_\xi}$ with $n_\xi = n_w + n_y + n_u$, and $\upsilon := (\dot{d}_y, \dot{d}_u) \in \mathbb{R}^{n_y + n_u}$. As in [2], the system can be modeled as the following hybrid system

$$\dot{q} = \begin{pmatrix} \mathcal{A}_1 x + \mathcal{B}_1 e_y + \mathcal{M}_1 e_u + \mathcal{E}_1 \xi \\ \mathcal{A}_2 x + \mathcal{M}_2 e_u + \mathcal{E}_2 \xi + \mathcal{F}_2 \upsilon \\ \mathcal{A}_3 x + \mathcal{B}_3 e_y + \mathcal{E}_3 \xi + \mathcal{F}_3 \upsilon \\ 1 \\ 1 \end{pmatrix} \quad q \in \mathcal{C}_y \cap \mathcal{C}_u$$

$$q^+ \in \begin{cases} \Big\{(x, 0, e_u, 0, \tau_u)\Big\} & q \in \mathcal{D}_y \backslash \mathcal{D}_u \\ \Big\{(x, e_y, 0, \tau_y, 0)\Big\} & q \in \mathcal{D}_u \backslash \mathcal{D}_y \\ \Big\{(x, 0, e_u, 0, \tau_u), (x, e_y, 0, \tau_y, 0)\Big\} & q \in \mathcal{D}_y \cap \mathcal{D}_u, \end{cases} \tag{5}$$

where $\mathcal{A}_1 := \begin{bmatrix} A_p & B_p C_c \\ B_c C_p & A_c \end{bmatrix}$, $\mathcal{B}_1 := \begin{bmatrix} 0 \\ B_c \end{bmatrix}$, $\mathcal{M}_1 := \begin{bmatrix} B_p \\ 0 \end{bmatrix}$, $\mathcal{E}_1 := \begin{bmatrix} E_p & 0 & B_p \\ 0 & B_c & 0 \end{bmatrix}$, $\mathcal{A}_2 = -C_y \mathcal{A}_1$, $\mathcal{M}_2 := -C_y \mathcal{M}_1$, $\mathcal{E}_2 := -C_y \mathcal{E}_1$, $\mathcal{F}_2 := \begin{bmatrix} -1 & 0 \end{bmatrix}$, $\mathcal{A}_3 = -C_u \mathcal{A}_1$, $\mathcal{B}_3 := -C_u \mathcal{B}_1$, $\mathcal{E}_3 := -C_u \mathcal{E}_1$, and $\mathcal{F}_3 := \begin{bmatrix} 0 & -1 \end{bmatrix}$.

The sets $\mathcal{C}_y, \mathcal{D}_y$ are defined according to the triggering condition for the output measurement y, and the sets $\mathcal{C}_u, \mathcal{D}_u$ are constructed based on the triggering condition for the control input u. The first two cases in the jump map in (5) correspond to the situations when only the triggering condition of the output measurements or of the control input is verified, respectively. The last case in the jump map describes the time instants when both triggering conditions are satisfied, i.e., when $t_i^y = t_j^u$ for some $i \in \mathcal{I}_y$ and $j \in \mathcal{I}_u$ [1]. We design the flow and the jump sets in (5) as follows (as in [2])

$$\begin{aligned} \mathcal{C}_y &:= \Big\{q : |e_y| \leq \rho_y |y| \text{ or } \tau_y \in [0, T_y]\Big\} \\ \mathcal{D}_y &:= \Big\{q : |e_y| \geq \rho_y |y| \text{ and } \tau_y \geq T_y\Big\} \\ \mathcal{C}_u &:= \Big\{q : |e_u| \leq \rho_u |u| \text{ or } \tau_u \in [0, T_u]\Big\} \\ \mathcal{D}_u &:= \Big\{q : |e_u| \geq \rho_u |u| \text{ and } \tau_u \geq T_u\Big\}, \end{aligned} \tag{6}$$

where $\rho_y, \rho_u \geq 0$ are design parameters. The constants $T_y \in (0, \mathcal{T}_y(\gamma_y))$ and $T_u \in (0, \mathcal{T}_u(\gamma_u))$ are the minimum times that we enforce between two consecutive transmission instants of the output measurement y and of the control input u, respectively, where

$$\mathcal{T}_y(\gamma_y) := \tfrac{1}{\gamma_y} \tfrac{\pi}{2}, \qquad \mathcal{T}_u(\gamma_u) := \tfrac{1}{\gamma_u} \tfrac{\pi}{2} \tag{7}$$

and γ_y and γ_u are designed in the sequel. The upper bounds $\mathcal{T}_y(\gamma_y), \mathcal{T}_u(\gamma_u)$ are related to *maximally allowable transmission intervals* (MATI) of time-triggered controllers in the context of sampled-data systems [19].

[1] The definition of G in this case ensures that it is outer semicontinuous, which is one of the hybrid basic conditions ensuring the well-posedness of system (5). This would not be the case if we would define $G(q)$ as $\{(x, 0, 0, 0, 0)\}$ when $q \in \mathcal{D}_y \cap \mathcal{D}_u$, see [2].

Remark 1 *The upper bounds $\mathcal{T}_y(\gamma_y), \mathcal{T}_u(\gamma_u)$ in (7) are obtained similarly to [19]. Although their values can subject to some conservatism, we only use those constant times to prevent the occurrence of Zeno at each channel, which is sufficient to the purpose of this study. Their expressions in (7) are simplified versions of those given in [2], see also [8]. This is due to the fact that the control input u in (3) does not involve a feedthrough term and that the plant output and the control input are transmitted asynchronously, which leads to $L_{y_1} = L_{u_1} = 0$ in (27) in [2].* □

We consider the following controlled output

$$z = [C_z^p \quad 0]x + [D_z^w \quad D_z^y \quad D_z^u]\xi := C_z x + D_z \xi, \tag{8}$$

where $C_z^p, D_z^w, D_z^y, D_z^u$ are matrices of appropriate dimensions.

The objective of this study is to synthesize both controller (3), i.e., the matrices A_c, B_c, C_c, and the flow and the jump sets in (6), i.e., the parameters ρ_y, ρ_u, T_y, T_u, such that system (5) is $\mathcal{L}_2$-stable from (ξ, υ) to z with a guaranteed $\mathcal{L}_2$-gain. We first revisit the emulation results of [2] for this purpose, then we develop the co-design procedure.

4 Emulation

In emulation, we first assume that a stabilizing feedback law (3) is already available and we only construct $\mathcal{C}_y, \mathcal{C}_u$ and $\mathcal{D}_y, \mathcal{D}_u$. We use boldface symbols to emphasize the LMIs decision variables.

Proposition 1 *Consider system (5) with the flow and the jump sets defined in (6) and the output z in (8). Assume that a stabilizing feedback law (3) is given. Suppose that there exist real scalars $\boldsymbol{\varepsilon}_y, \boldsymbol{\varepsilon}_u, \boldsymbol{\mu}_y, \boldsymbol{\mu}_u, \boldsymbol{\vartheta}_\xi, \boldsymbol{\vartheta}_\upsilon > 0$, $\boldsymbol{\lambda}_y, \boldsymbol{\lambda}_u \in (0, 1)$ and a positive definite symmetric real matrix $\boldsymbol{P}$ such that (8) holds, where $D_y := [0 \ 1 \ 0]$ and $D_u := [0 \ 0 \ 1]$. Let the parameters of the event-triggering mechanism (6) and of the times $\mathcal{T}_y(\gamma_y), \mathcal{T}_u(\gamma_u)$ in (7) be selected as $\rho_y = \frac{\sqrt{\varepsilon_y}}{\lambda_y \gamma_y}$, $\rho_u = \frac{\sqrt{\varepsilon_u}}{\lambda_u \gamma_u}$ with $\lambda_y = \sqrt{\boldsymbol{\lambda}_y}$, $\lambda_u = \sqrt{\boldsymbol{\lambda}_u}$, $\gamma_y = \sqrt{\frac{\boldsymbol{\mu}_y}{\boldsymbol{\lambda}_y}}$, $\gamma_u = \sqrt{\frac{\boldsymbol{\mu}_u}{\boldsymbol{\lambda}_u}}$, $\varepsilon_y = \boldsymbol{\varepsilon}_y$ and $\varepsilon_y = \boldsymbol{\varepsilon}_u$. Then, system (5), (6) is $\mathcal{L}_2$-stable from (ξ, υ) to z with an $\mathcal{L}_2$-gain less than or equal to $\eta := \sqrt{\max\{\boldsymbol{\vartheta}_\xi, \boldsymbol{\vartheta}_\upsilon\}}$.* □

The proof of Proposition 1 follows similar lines as in the proof of Proposition 1 in [2] and as in Section VI-C in [8], it is therefore omitted. The decision variables $\boldsymbol{\varepsilon}_y, \boldsymbol{\varepsilon}_u, \boldsymbol{\mu}_y, \boldsymbol{\mu}_u, \boldsymbol{\lambda}_y, \boldsymbol{\lambda}_u$ are used to determine the transmission parameters of the event-triggering mechanism (6), i.e., the triggering threshold parameters ρ_y, ρ_u and

$$\begin{pmatrix} \Omega_{11} & \star & \star & \star & \star \\ \mathcal{B}_1^T\boldsymbol{P}+\boldsymbol{\lambda}_u\mathcal{B}_3^T\mathcal{A}_3 & \boldsymbol{\lambda}_u\mathcal{B}_3^T\mathcal{B}_3-\boldsymbol{\mu}_y\mathbb{I}_{n_y} & \star & \star & \star \\ \mathcal{M}_1^T\boldsymbol{P}+\boldsymbol{\lambda}_y\mathcal{M}_2^T\mathcal{A}_2 & 0 & \boldsymbol{\lambda}_y\mathcal{M}_2^T\mathcal{M}_2-\boldsymbol{\mu}_u\mathbb{I}_{n_u} & \star & \star \\ \Omega_{41} & \boldsymbol{\lambda}_u\mathcal{E}_3^T\mathcal{B}_3 & \boldsymbol{\lambda}_y\mathcal{E}_2^T\mathcal{M}_2 & \Omega_{44} & \star \\ \boldsymbol{\lambda}_y\mathcal{F}_2^T\mathcal{A}_2+\boldsymbol{\lambda}_u\mathcal{F}_3^T\mathcal{A}_3 & \boldsymbol{\lambda}_u\mathcal{F}_3^T\mathcal{B}_3 & \boldsymbol{\lambda}_y\mathcal{F}_2^T\mathcal{M}_2 & \boldsymbol{\lambda}_y\mathcal{F}_2^T\mathcal{E}_2+\boldsymbol{\lambda}_u\mathcal{F}_3^T\mathcal{E}_3 & \boldsymbol{\lambda}_y\mathcal{F}_2^T\mathcal{F}_2+\boldsymbol{\lambda}_u\mathcal{F}_3^T\mathcal{F}_3-\boldsymbol{\vartheta}_v\mathbb{I}_{n_v} \end{pmatrix} < 0, \quad (8)$$

$$\begin{aligned} \Omega_{11} &:= \mathcal{A}_1^T\boldsymbol{P}+\boldsymbol{P}\mathcal{A}_1+C_z^TC_z+\boldsymbol{\lambda}_y\mathcal{A}_2^T\mathcal{A}_2+\boldsymbol{\lambda}_u\mathcal{A}_3^T\mathcal{A}_3+\boldsymbol{\varepsilon}_yC_y^TC_y+\boldsymbol{\varepsilon}_uC_u^TC_u \\ \Omega_{41} &:= \mathcal{E}_1^T\boldsymbol{P}+D_z^TC_z+\boldsymbol{\lambda}_y\mathcal{E}_2^T\mathcal{A}_2+\boldsymbol{\lambda}_u\mathcal{E}_3^T\mathcal{A}_3+\boldsymbol{\varepsilon}_yD_y^TC_y+\boldsymbol{\varepsilon}_uD_u^TC_u \\ \Omega_{44} &:= D_z^TD_z+\boldsymbol{\lambda}_y\mathcal{E}_2^T\mathcal{E}_2+\boldsymbol{\lambda}_u\mathcal{E}_3^T\mathcal{E}_3+\boldsymbol{\varepsilon}_yD_y^TD_y+\boldsymbol{\varepsilon}_uD_u^TD_u-\boldsymbol{\vartheta}_\xi\mathbb{I}_{n_\xi}. \end{aligned}$$

the enforced lower bounds T_y, T_u. In particular, the decision variables $\boldsymbol{\vartheta}_\xi, \boldsymbol{\vartheta}_v$ define the guaranteed $\mathcal{L}_2$-gain η. The parameters γ_y and γ_u are related to the $\mathcal{L}_2$-gains with which e_y and e_u affect the x-system. Smaller values of γ_y, γ_u leads to smaller $\mathcal{L}_2$-gains and larger bounds $\mathcal{T}_y, \mathcal{T}_u$, respectively, and vice versa, in view of (7). Finally, the parameters λ_y, λ_u and $\varepsilon_y, \varepsilon_u$ are introduced to relax condition (8); we could have stated (8) with $\varepsilon_y = \varepsilon_u = 1$ and $\lambda_y = \lambda_u = 1$, but this leads to a more conservative condition.

The guaranteed $\mathcal{L}_2$-stability in Proposition 1 is from the disturbances (ξ, v) to z with v is the derivative of the measurement noises (d_y, d_u). The dependence of the $\mathcal{L}_2$-gain on v is because of the sampling of the noisy measurements of the plant output and the control input, see (2), (3) and the definitions of the sampling-induced errors e_y, e_u. As a result, the dynamics of e_y and e_u between two transmission instants of the plant output and of the control input, respectively, will depend on the derivatives $\dot{d}_y$ and $\dot{d}_u$ of the measurement noise. Similar type of results have naturally appeared in, e.g., sampled-data systems [18] and hybrid dynamical systems [24].

It is important to mention that condition (8) represents an LMI constraint only if the controller matrices A_c, B_c, C_c are known. When this is not the case, nonlinear terms appear in (8) such as $\mathcal{A}_2^T\mathcal{A}_2$ and $\mathcal{A}_3^T\mathcal{A}_3$ in Ω_{11}, since $\mathcal{A}_2, \mathcal{A}_3$ depend on the controller matrices, in view of their definition after (5). The encountered nonlinearities in this case are not trivial to handle and cannot be resolved by standard congruence transformations due to the presence of non-invertible matrices, as shown in the proof of forthcoming Theorem 3. This forms one of the main challenges in this study.

Remark 2 *Proposition 1 exhibits substantial differences compared to Proposition 1 in [2]. First, the exogenous inputs are concatenated in two vectors ξ, v and not in one vector as in [2]. This modeling choice allows to resolve some nonlinearities that appear in (8) when the controller is no longer known. Second, the effect of the sampling induced errors e_y and e_u on each other is handled in [2] by the event-triggering rules, see (24) in [2]. Alternatively, the interaction between e_y and e_u in this study is dealt with the time-triggering rules. This design choice leads to $L_{y_2} = L_{u_2} = 0$ in (24) in [2], which further simplifies the co-design procedure, see Section V in [1]. Besides the benefits on the co-design analysis, the above differences also highlight the flexibility of the proposed event-triggering scheme in [2].* □

5 LMI for co-design

5.1 Main result

We present the co-design procedure for the general case where both the plant output and the control input are transmitted asynchronously, which relies on the next result.

Theorem 3 *Consider system (5) with the flow and the jump sets defined in (6) and the output z in (8). Suppose that for given real scalars $\lambda_y, \lambda_u \in (0,1), \vartheta_\xi, \vartheta_v > 0$, there exist symmetric positive definite real matrices $\boldsymbol{X}, \boldsymbol{Y} \in \mathbb{R}^{n_p \times n_p}$, real matrices $\boldsymbol{M} \in \mathbb{R}^{n_p \times n_p}, \boldsymbol{Z} \in \mathbb{R}^{n_p \times n_y}, \boldsymbol{N} \in \mathbb{R}^{n_u \times n_p}$ and real scalars $\boldsymbol{\mu}_y, \boldsymbol{\mu}_u, \boldsymbol{\sigma}_y, \boldsymbol{\sigma}_u > 0$ such that (9), (10) are satisfied, where $\widetilde{\vartheta}_v := \vartheta_v - \max\{\lambda_y^2, \lambda_u^2\}$ in (9). Let the dynamic controller (3) be given by*

$$\begin{aligned} A_c &= V^{-1}(\boldsymbol{M} - \boldsymbol{Y}A_p\boldsymbol{X} - \boldsymbol{Y}B_p\boldsymbol{N} - \boldsymbol{Z}C_p\boldsymbol{X})U^{-T} \\ B_c &= V^{-1}\boldsymbol{Z}, \qquad C_c = \boldsymbol{N}U^{-T}, \end{aligned} \tag{11}$$

with $U, V \in \mathbb{R}^{n_p \times n_p}$ any square and invertible matrices such that[2] $UV^T = \mathbb{I}_{n_p} - \boldsymbol{XY}$. Select the parameters of the event-triggering mechanism (6) such that $\rho_y = \frac{\sqrt{\varepsilon_y}}{\lambda_y\gamma_y}$, $\rho_u = \frac{\sqrt{\varepsilon_u}}{\lambda_u\gamma_u}$ with $\gamma_y = \frac{\sqrt{\boldsymbol{\mu}_y}}{\lambda_y}$, $\gamma_u = \frac{\sqrt{\boldsymbol{\mu}_u}}{\lambda_u}$, $\varepsilon_y = \boldsymbol{\sigma}_y^{-1}$ and $\varepsilon_u = \boldsymbol{\sigma}_u^{-1}$. Then, system (5), (6) is $\mathcal{L}_2$-stable from (ξ, v) to z with an $\mathcal{L}_2$-gain less than or equal to $\eta = \sqrt{\max\{\vartheta_\xi, \vartheta_v\}}$. □

[2] In view of the Schur complement of (10), we deduce that $\begin{pmatrix} \boldsymbol{Y} & \mathbb{I}_{n_p} \\ \mathbb{I}_{n_p} & \boldsymbol{X} \end{pmatrix} > 0$, which implies that $\boldsymbol{X} - \boldsymbol{Y}^{-1} > 0$ and thus $\mathbb{I}_{n_p} - \boldsymbol{XY}$ is nonsingular. Hence, the existence of nonsingular matrices U, V, which is needed in view of (11), is always ensured.

$$
\begin{pmatrix}
\boldsymbol{\Gamma}_1+\boldsymbol{\Gamma}_1^T & \star & \star & \star & \star & \star & \star & \star & \star & \star \\
\tilde{\boldsymbol{Z}}^T & -\boldsymbol{\mu}_y\mathbb{I}_{n_y} & \star & \star & \star & \star & \star & \star & \star & \star \\
\tilde{\boldsymbol{Y}}^T & 0 & -\boldsymbol{\mu}_u\mathbb{I}_{n_u} & \star & \star & \star & \star & \star & \star & \star \\
\boldsymbol{\Gamma}_2^T & 0 & 0 & -\vartheta_\xi\mathbb{I}_{n_\xi} & \star & \star & \star & \star & \star & \star \\
\boldsymbol{\Gamma}_1 & \tilde{\boldsymbol{Z}} & \tilde{\boldsymbol{Y}} & \boldsymbol{\Gamma}_2 & -\widetilde{\vartheta}_v\boldsymbol{\Gamma}_3 & \star & \star & \star & \star & \star \\
\boldsymbol{\Gamma}_1 & 0 & \tilde{\boldsymbol{Y}} & \boldsymbol{\Gamma}_2 & 0 & -\lambda_y^{-2}\boldsymbol{\Gamma}_3 & \star & \star & \star & \star \\
\boldsymbol{\Gamma}_1 & \tilde{\boldsymbol{Z}} & 0 & \boldsymbol{\Gamma}_2 & 0 & 0 & -\lambda_u^{-2}\boldsymbol{\Gamma}_3 & \star & \star & \star \\
\tilde{\boldsymbol{X}}_p & 0 & 0 & D_y & 0 & 0 & 0 & -\boldsymbol{\sigma}_y\mathbb{I}_{n_y} & \star & \star \\
\tilde{\boldsymbol{N}} & 0 & 0 & D_u & 0 & 0 & 0 & 0 & -\boldsymbol{\sigma}_u\mathbb{I}_{n_u} & \star \\
\tilde{\boldsymbol{X}}_z & 0 & 0 & D_z & 0 & 0 & 0 & 0 & 0 & -\mathbb{I}_{n_z}
\end{pmatrix} < 0 \tag{9}
$$

$$
\begin{pmatrix}
-\mathbb{I}_{n_y} & \star & \star \\
0 & -\mathbb{I}_{n_u} & \star \\
-\lambda_y^2\tilde{\boldsymbol{X}}_p^T & -\lambda_u^2\tilde{\boldsymbol{N}}^T & -\boldsymbol{\Gamma}_3
\end{pmatrix} < 0, \qquad
\begin{pmatrix}
-\mathbb{I}_{n_y} & \star \\
-\tilde{\boldsymbol{X}}_p^T & -\boldsymbol{\Gamma}_3
\end{pmatrix} < 0, \qquad
\begin{pmatrix}
-\mathbb{I}_{n_u} & \star \\
-\tilde{\boldsymbol{N}}^T & -\boldsymbol{\Gamma}_3
\end{pmatrix} < 0, \tag{10}
$$

$$
\boldsymbol{\Gamma}_1 := \begin{pmatrix} \boldsymbol{Y}A_p + \boldsymbol{Z}C_p & \boldsymbol{M} \\ A_p & A_p\boldsymbol{X} + B_p\boldsymbol{N} \end{pmatrix}, \quad
\boldsymbol{\Gamma}_2 := \begin{pmatrix} \boldsymbol{Y}E_p & \boldsymbol{Z} & \boldsymbol{Y}B_p \\ E_p & 0 & B_p \end{pmatrix}, \quad
\boldsymbol{\Gamma}_3 := \begin{pmatrix} \boldsymbol{Y} & \mathbb{I}_{n_p} \\ \mathbb{I}_{n_p} & \boldsymbol{Y} \end{pmatrix}, \quad
\tilde{\boldsymbol{Z}} := \begin{pmatrix} \boldsymbol{Z} \\ 0 \end{pmatrix}
$$

$$
\tilde{\boldsymbol{Y}} := \begin{pmatrix} \boldsymbol{Y}B_p \\ B_p \end{pmatrix}, \qquad
\tilde{\boldsymbol{X}}_p := (C_p \;\; C_p\boldsymbol{X}), \qquad
\tilde{\boldsymbol{X}}_z := (C_z^p \;\; C_z^p\boldsymbol{X}), \qquad
\tilde{\boldsymbol{N}} := (0 \;\; \boldsymbol{N}).
$$

The proof of Theorem 3 consists of showing that the feasibility of (9)-(10) leads to (8), which in turn implies the $\mathcal{L}_2$-stability of the hybrid system (5), (6) according to Proposition 1. To obtain the LMI conditions (9)-(10), we rely on the following facts. First, we used the property that condition (8) is symmetric and that we do not consider the feedthrough term in (3). Second, we applied the change of variables technique, inspired by [22], to handle some nonlinear terms, as shown in the proof of Theorem 3. Third, we introduced the additional constraints in (10) to overcome other nonlinear terms that could not be solved by standard techniques. We explain in the next section how to exploit Theorem 3 to optimize properties of the transmission times.

Remark 3 *The co-design procedure generates a tradeoff between the upper-bound η on the $\mathcal{L}_2$-gain and the guaranteed minimum times T_y, T_u. As mentioned before, the feasibility of (9)-(10) leads to (8). The feasibility of (8) in turn can be only guaranteed if the diagonal entries in (8) are negative, which will be the case when the values of $\boldsymbol{\lambda}_y, \boldsymbol{\lambda}_u, \boldsymbol{\varepsilon}_y, \boldsymbol{\varepsilon}_u$ are sufficiently small and the values of $\boldsymbol{\vartheta}_\xi, \boldsymbol{\vartheta}_v$ are sufficiently large. Consequently, this creates an intuitive tradeoff between the transmission parameters $\boldsymbol{\lambda}_y, \boldsymbol{\lambda}_u, \boldsymbol{\varepsilon}_y, \boldsymbol{\varepsilon}_u$ and the upper-bound η on the $\mathcal{L}_2$-gain, in view of (7) and the definition of η in Theorem 3. In other words, smaller values of $\boldsymbol{\lambda}_y, \boldsymbol{\lambda}_u$ lead to larger values of the MATI bounds $\mathcal{T}_y, \mathcal{T}_u$. However, the estimated $\mathcal{L}_2$-gain η might increase, and vice versa.* □

5.2 Time-triggered control

Our co-design results are also relevant and new for time-triggered control. In this case, the flow and the jump sets in (6) become

$$
\mathcal{C}_y = \{q : \tau_y \in [0, T_y]\}, \quad \mathcal{D}_y = \{q : \tau_y \in [\epsilon_y, T_y]\}
$$
$$
\mathcal{C}_u = \{q : \tau_u \in [0, T_u]\}, \quad \mathcal{D}_u = \{q : \tau_u \in [\epsilon_u, T_u]\},
$$

where $\epsilon_y \in (0, T_y]$, $\epsilon_u \in (0, T_u]$ are introduced to prevent Zeno behaviour, and T_y, T_u are strictly smaller than $\mathcal{T}_y(\gamma_y)$, $\mathcal{T}_u(\gamma_u)$ defined in (7). When $\epsilon_y = T_y$ and $\epsilon_u = T_u$, the sets in (6) lead to periodic and asynchronous transmissions of the output measurement and of the control input, respectively. Hence, the co-design problem reduces to jointly synthesizing the dynamic controller (3) and the times T_y, T_u. Then, the conclusion of Theorem 3 holds, by following similar lines as in the proof of Theorem 3, when conditions (9)-(10) are verified. Note that in the case of time-triggered control, the parameters σ_y, σ_u in (9) are not needed since we do not have the event-triggering rules $|e_y| \geq \rho_y|y|$, $|e_u| \geq \rho_u|u|$ in this case and thus condition (9) can be relaxed by eliminating the $8th$ and the $9th$ rows and columns from (9).

6 Optimization problems

We first exploit the results of Section 5 to enlarge the guaranteed minimum times T_y, T_u between two successive transmissions at each channel. We then propose a heuristic method to reduce the amount of transmissions.

6.1 Enlarging the minimum inter-transmission times

The enforced minimum times T_y, T_u are a priori only lower bounds on the inter-transmission times. The next lemma reveals that these are actually the minimum inter-transmission times for the transmission instants of the output measurement and of the control input, respectively.

Lemma 1 *For any $q_0 \in \mathcal{C} \cup \mathcal{D}$, let $\mathcal{S}(q_0)$ be the set of solution pairs (ϕ_q, ϕ_ξ) to system (5), (6) with $\phi_q(0,0) = q_0$. For a solution (ϕ_q, ϕ_ξ), we denote by (t_{j_y}, j_y) with $j_y \in \mathbb{Z}_{>0}$ the hybrid times such that $\phi_q(t_{j_y}, j_y) \in \mathcal{D}_y$ and $\phi_q(t_{j_y}, j_y+1) \notin \mathcal{D}_y$. Similarly, for a solution (ϕ_q, ϕ_ξ), we denote by (t_{j_u}, j_u) with $j_u \in \mathbb{Z}_{>0}$ the hybrid times such that $\phi_q(t_{j_u}, j_u) \in \mathcal{D}_u$ and $\phi_q(t_{j_u}, j_u+1) \notin \mathcal{D}_u$, respectively. Then, for any $q_0 \in \mathcal{C} \cup \mathcal{D}$, there exists $(\phi_q, \phi_\xi^*) \in \mathcal{S}(q_0)$ and $T_y = \min\{t_{j_y+1} - t_{j_y} : \exists j_y \in \mathbb{Z}_{>0},\ (t_{j_y}, j_y), (t_{j_y}, j_y+1), (t_{j_y+1}, j_y+1), (t_{j_y+1}, j_y+2) \in \operatorname{dom}\phi_q\}$ and $T_u = \min\{t_{j_u+1} - t_{j_u} : \exists j_u \in \mathbb{Z}_{>0},\ (t_{j_u}, j_u), (t_{j_u}, j_u+1), (t_{j_u+1}, j_u+1), (t_{j_u+1}, j_u+2) \in \operatorname{dom}\phi_q\}$.* □

Lemma 1 means that for any initial condition, we can find certain exogenous inputs w, d_y, d_u such that the minimum time elapsed between two successive transmissions of the plant output and of the control input over the solution to system (5), (6) is exactly T_y and T_u, respectively. This consequently means that T_y and T_u are the actual minimum inter-transmission times of the output measurement y and of the control input u, respectively.

In order to enlarge T_y, T_u, we need to enlarge $\mathcal{T}_y(\gamma_y)$, $\mathcal{T}_u(\gamma_u)$. For this purpose, in view of (7), we need to minimize γ_y, γ_u, given $\lambda_y, \lambda_u \in (0,1)$. Since $\gamma_y = \frac{\sqrt{\mu_y}}{\lambda_y}$, $\gamma_u = \frac{\sqrt{\mu_u}}{\lambda_u}$ and μ_y, μ_u are decision variables of (9), (10). This multi-objective problem can be addressed by solving the following problem, for fixed values of $\lambda_y, \lambda_u, \vartheta_\xi, \vartheta_\upsilon$

$$\begin{gathered}\min \delta_1 \mu_y + \delta_2 \mu_u \\ \text{subject to (9), (10)}\end{gathered} \tag{12}$$

for some weights $\delta_1, \delta_2 \geq 0$.

6.2 Reducing the amount of transmissions

While enlarging T_y, T_u can be useful to increase the guaranteed minimum times between two transmission instants of the plant output and of the control input, respectively, this may not necessarily lead to a further reduction in the average amount of transmissions. For the last purpose, a heuristic way to proceed is to maximize the parameters ρ_y, ρ_u of the event-triggering rules in (6).

In view of (6), the event-triggering rule of the output measurement y is $|e_y| \geq \rho_y |y|$. Since $\rho_y = \frac{\sqrt{\varepsilon_y}}{\lambda_y \gamma_y}$, then minimizing γ_y, by minimizing μ_y in (9)-(10), and maximizing ε_y, by minimizing σ_y, σ_u in (9)-(10) may result in enlarging the time it takes for event-triggering rule to be violated, i.e., that may enlarge the inter-transmission times, see Remark 4 below for further insights. Similar arguments apply for reducing the amount of transmissions of the control input u.

Since $\varepsilon_y = \sigma_y^{-1}, \varepsilon_u = \sigma_u^{-1}$ and σ_y, σ_u are decision variables of (9)-(10), we solve this problem by implementing the following algorithm, for fixed values of $\lambda_y, \lambda_u, \vartheta_\xi, \vartheta_\upsilon$

$$\begin{gathered}\min \delta_1 \mu_y + \delta_2 \mu_u + \delta_3 \sigma_y + \delta_4 \sigma_u \\ \text{subject to (9), (10)}\end{gathered} \tag{13}$$

for some weights $\delta_1, \delta_2, \delta_3, \delta_4 \geq 0$.

Remark 4 *When we optimize the parameters γ_y, γ_u, ε_y, ε_u, the obtained controller matrices A_c, B_c, C_c will consequently be changed. As a result, even if ρ_y and ρ_u are maximized, the dynamics of e_y and e_u will be different and it may be the case that these reach their thresholds $\rho_y|y|$ and $\rho_u|u|$, respectively, faster so that the inter-transmission times are not necessarily larger. That is the reason why the method in this subsection is heuristic. The simulation results in Section 7 show that this does not occur for the considered example and that the optimization problem (13) can greatly reduce the amount of transmissions.* □

7 Illustrative example

Consider the plant model in Example 3 in [9] affected by external disturbances and measurement noises, where the plant matrices are given by $A_p = \begin{bmatrix} 0 & 1 \\ -2 & -3 \end{bmatrix}$, $B_p = \begin{bmatrix} 0 & 1 \end{bmatrix}^T$, $E_p = \begin{bmatrix} 0 & 1 \end{bmatrix}^T$, $C_p = \begin{bmatrix} 1 & 0 \end{bmatrix}$. We consider $C_z^p = \begin{bmatrix} 1 & 0.5 \end{bmatrix}$ and $D_z = \begin{bmatrix} 0.5 & 0 & 0 \end{bmatrix}$ for the performance output z in (8). We first apply the emulation approach in Section 4 with the controller given in [9] and then we implement the co-design algorithm and we compare the obtained results. We affect the system by exogenous inputs w, d_y, d_u satisfying $|w(t,j)| \leq 0.5$, $d_y(t,j) = 0.1\sin(50t)$ and $d_u(t,j) = 0.01\sin(50t)$. We run simulations for 5 seconds with 100 initial conditions such that $x(0,0)$ is randomly distributed in a ball of radius 100, $e(0,0) = (0,0)$ and $\tau(0,0) = (0,0)$. The guaranteed $\mathcal{L}_2$-gain η using the emulated controller is $\eta = 1.0195$ and the guaranteed lower bounds T_y and T_u are shown in Table 1. Then, we apply the co-design procedure in Section 5. We found that conditions (9), (10) are feasible with $\eta = 1.1832$, which is slightly larger than the value obtained by emulation. However, the enforced lower bounds T_y and T_u have been enlarged by more than 50000% and 8000%, respectively, using the optimization algorithms (12) with $\delta_1 = \delta_2 = 1$ and (13) with $\delta_i = 1, i \in \{1, \ldots, 4\}$ as shown in Table 1. In this case, the optimization algorithm (12) leads to almost periodic sampling, since $\tau^y_{\text{avg}} \approx T_y$ and $\tau^u_{\text{avg}} \approx T_u$. This behaviour is justified by the fact that the obtained values of γ_y, γ_u are very large compared to the values of $\varepsilon_y, \varepsilon_u$, respectively, which lead to very

$$\begin{pmatrix}
\mathcal{A}_1^T P + P\mathcal{A}_1 & \star & \star & \star & \star & \star & \star & \star & \star & \star \\
\mathcal{B}_1^T P & -\mu_y \mathbb{I}_{n_y} & \star & \star & \star & \star & \star & \star & \star & \star \\
\mathcal{M}_1^T P & 0 & -\mu_u \mathbb{I}_{n_u} & \star & \star & \star & \star & \star & \star & \star \\
\mathcal{E}_1^T P & 0 & 0 & -\vartheta_\xi \mathbb{I}_{n_\xi} & \star & \star & \star & \star & \star & \star \\
G\mathcal{A}_1 & G\mathcal{B}_1 & G\mathcal{M}_1 & G\mathcal{E}_1 & -\widetilde{\vartheta}_v GSG^T & \star & \star & \star & \star & \star \\
-C_y\mathcal{A}_1 & 0 & -C_y\mathcal{M}_1 & -C_y\mathcal{E}_1 & 0 & -\lambda_y^{-2} C_y S C_y^T & \star & \star & \star & \star \\
-C_u\mathcal{A}_1 & -C_u\mathcal{B}_1 & 0 & -C_u\mathcal{E}_1 & 0 & 0 & -\lambda_u^{-2} C_u S C_u^T & \star & \star & \star \\
C_y & 0 & 0 & D_y & 0 & 0 & 0 & -\sigma_y \mathbb{I}_{n_y} & \star & \star \\
C_u & 0 & 0 & D_u & 0 & 0 & 0 & 0 & -\sigma_u \mathbb{I}_{n_u} & \star \\
C_z & 0 & 0 & D_z & 0 & 0 & 0 & 0 & 0 & -\mathbb{I}_{n_z}
\end{pmatrix} < 0. \tag{14}$$

small values of $\rho_y = \frac{\sqrt{\varepsilon_y}}{\lambda_y \gamma_y}$ and $\rho_u = \frac{\sqrt{\varepsilon_u}}{\lambda_u \gamma_u}$. This consequently leads to quick violations of the event-triggering rules $|e_y| \leq \rho_y |y|$ and $|e_u| \leq \rho_u |u|$. We have then used the results of Section 6.2 to overcome this issue, which resulted in $\tau^y_{\text{avg}} > \tau^y_{\min}$ and $\tau^u_{\text{avg}} > \tau^u_{\min}$, as shown in third line of Table 1. We emphasize that the obtained results depend on the choice of the weights $\delta_i, i \in \{1, \dots, 4\}$, and that different choices will lead to different performances. The controller matrices in (3) for the last case in Table 1 are

	T_y	τ^y_{avg}	T_u	τ^u_{avg}
Emulation: Proposition 1	5.9483×10^{-5}	6.6127×10^{-5}	1.3197×10^{-4}	1.4672×10^{-4}
Optimization 1: (12)	0.0736	0.0737	0.0175	0.0176
Optimization 2: (13)	0.0388	0.1594	0.0125	0.0589

Table 1
Comparison between emulation and co-design.

$$A_c = \begin{bmatrix} -2.0964 & 0.6938 \\ -0.9671 & -0.9093 \end{bmatrix}, B_c = \begin{bmatrix} 5.4891 \\ 3.3864 \end{bmatrix}, C_c = \begin{bmatrix} -0.0459 \\ 0.0404 \end{bmatrix}^T.$$

8 Conclusion

We have investigated the joint design of dynamic output feedback laws and event-triggering conditions for linear systems subject to exogenous inputs. Sufficient conditions have been provided, in terms of LMIs, to ensure an $\mathcal{L}_2$-stability property for the closed-loop system. Two optimization algorithms have been presented to enlarge the enforced lower bounds on the inter-transmission times and/or to reduce the average amount of transmissions. The effectiveness of the approach has been illustrated on a numerical example.

Appendix

Proof of Theorem 3. We define the following matrices

$$S = \begin{pmatrix} X & U \\ U^T & \hat{X} \end{pmatrix}, \; S^{-1} = \begin{pmatrix} Y & V \\ V^T & \hat{Y} \end{pmatrix}, \; \Gamma = \begin{pmatrix} Y & \mathbb{I}_{n_p} \\ V^T & 0 \end{pmatrix},$$

where $\hat{X}, \hat{Y} \in \mathbb{R}^{n_p \times n_p}$ are symmetric positive definite real matrices of appropriate dimension. Since $SS^{-1} = \mathbb{I}_{2n_p}$, it holds that $XY + UV^T = U^T V + \hat{X}\hat{Y} = \mathbb{I}_{n_p}$ and $XV + U\hat{Y} = U^T Y + \hat{X} V^T = 0$. We also introduce the following matrix $G = \begin{pmatrix} \lambda_y^2 C_p & 0 \\ 0 & \lambda_u^2 C_c \end{pmatrix}$. After some direct calculations, in view of (11), we obtain (recall that $C_y = [C_p \;\; 0], C_u = [0 \;\; C_c], C_z = [C_z^p \;\; 0]$)

$$S\Gamma = \begin{pmatrix} \mathbb{I}_{n_p} & X \\ 0 & U^T \end{pmatrix}, \;\; GS\Gamma = \begin{pmatrix} \lambda_y^2 \tilde{X}_p \\ \lambda_u^2 \tilde{N} \end{pmatrix}, \;\; \Gamma^T S \Gamma = \Gamma_3,$$

$$\mathcal{B}_1^T \Gamma = \tilde{Z}^T, \;\; \mathcal{M}_1^T \Gamma = \tilde{Y}^T, \;\; \mathcal{E}_1^T \Gamma = \Gamma_2, \;\; \Gamma^T \mathcal{A}_1 S \Gamma = \Gamma_1$$

$$C_y S \Gamma = \tilde{X}_p, \;\; C_u S \Gamma = \tilde{N}, \;\; C_z S \Gamma = \tilde{X}_z.$$

By substituting the above equalities in (9), (10), then multiplying (9) from the left by diag$\{S^{-1}\Gamma^{-T}, 1, 1, 1, G\Gamma^{-T}, -C_y\Gamma^{-T}, -C_u\Gamma^{-T}, 1, 1, 1\}$ and from the right by diag$\{\Gamma^{-1}S^{-1}, 1, 1, 1, \Gamma^{-1}G^T, -\Gamma^{-1}C_y^T, -\Gamma^{-1}C_u^T, 1, 1, 1\}$ and by taking $P = S^{-1}$, we obtain (14). In view of the Schur complement of (10), it holds that

$$-\mathbb{I}_{n_v} < -GSG^T, \; -\mathbb{I}_{n_y} < -C_y S C_y^T, \; -\mathbb{I}_{n_u} < -C_u S C_u^T. \tag{15}$$

Note also that $\mathcal{A}_2 = -C_y\mathcal{A}_1$, $\mathcal{M}_2 = -C_y\mathcal{M}_1$, $\mathcal{E}_2 = -C_y\mathcal{E}_1$, $\mathcal{A}_3 = -C_u\mathcal{A}_1$, $\mathcal{B}_3 = -C_u\mathcal{B}_1$, $\mathcal{E}_3 = -C_u\mathcal{E}_1$. Moreover, in view of (5) and the definition of the matrix G, we have that $G\mathcal{A}_1 = \lambda_y^2 \mathcal{F}_2^T \mathcal{A}_2 + \lambda_u^2 \mathcal{F}_3^T \mathcal{A}_3$, $G\mathcal{B}_1 = \lambda_u^2 \mathcal{F}_3^T \mathcal{B}_3$, $G\mathcal{M}_1 = \lambda_y^2 \mathcal{F}_2^T \mathcal{M}_2$, $G\mathcal{E}_1 = \lambda_y^2 \mathcal{F}_2^T \mathcal{E}_2 + \lambda_u^2 \mathcal{F}_3^T \mathcal{E}_3$ and $-\widetilde{\vartheta}_v \mathbb{I}_{n_v} = -\vartheta_v \mathbb{I}_{n_v} + \lambda_y^2 \mathcal{F}_2^T \mathcal{F}_2 + \lambda_u^2 \mathcal{F}_3^T \mathcal{F}_3$. By using (15) and the above equalities in (14) and then by applying the Schur complement (recall that $\varepsilon_y = \sigma_y^{-1}$ and $\varepsilon_u = \sigma_u^{-1}$), we deduce that (14) leads to (8). Thus, by virtue of Proposition 1, the $\mathcal{L}_2$-stability of system (5) is concluded with a guaranteed $\mathcal{L}_2$-gain $\eta = \sqrt{\max\{\boldsymbol{\vartheta}_\xi, \boldsymbol{\vartheta}_v\}}$. □

Proof of Lemma 1. Let $q_0 \in C \cup D$ and ϕ_q be a hybrid arc such that $\phi_q(0,0) = q_0$. Define $\phi_\xi = (0, -C_y\phi_x, -C_u\phi_x)$. The definitions of the flow and the jump sets in (6) guarantee that $\tau_{\min}^y \geq T_y$ and $\tau_{\min}^u \geq T_u$. We now show that $\tau_{\min}^y \leq T_y$ and $\tau_{\min}^u \leq T_u$. Since $\phi_{d_y}(t,j) = -C_y\phi_x(t,j)$ for all $(t,j) \in \operatorname{dom}\phi_q$, we have that $\phi_y(t,j_y) = C_y\phi_x(t,j_y) + \phi_{d_y}(t,j_y) = 0$, see (2), for all $(t,j_y) \in \operatorname{dom}\phi_q$. Then, it holds that $|\phi_{e_y}(t,j_y)| \geq \rho_y|\phi_y(t,j_y)| = 0$ for all $(t,j_y) \in \operatorname{dom}\phi_q$. As a result, $t_{j_y+1} = t_{j_y} + T_y$. Hence, two successive jumps of the plant output are separated by T_y units of time. Similar arguments apply for the inter-jump times of the control input u. Consequently, $T_y \geq \tau_{\min}^y$ and $T_u \geq \tau_{\min}^u$. We have shown that $T_y = \tau_{\min}^y$ and $T_u = \tau_{\min}^u$. $\square$

References

[1] M. Abdelrahim, R. Postoyan, J. Daafouz, and D. Nešić. Co-design of output feedback laws and event-triggering conditions for linear systems. *In Proceedings of the 53rd IEEE Conference on Decision and Control, Los Angeles, U.S.A.*, pages 3560–3565, 2014.

[2] M. Abdelrahim, R. Postoyan, J. Daafouz, and D. Nešić. Robust event-triggered output feedback controllers for nonlinear systems. *Automatica*, 75:96–108, 2017.

[3] F.D. Brunner, M. Heemels, and F. Allgöwer. Robust self-triggered MPC for constrained linear systems: A tube-based approach. *Automatica*, 72:73–83, 2016.

[4] C. Cai and A.R. Teel. Characterizations of input-to-state stability for hybrid systems. *Systems & Control Letters*, 58(1):47–53, 2009.

[5] D. Chwa. Fuzzy adaptive output feedback tracking control of VTOL aircraft with uncertain input coupling and input-dependent disturbances. *IEEE Transactions on Fuzzy Systems*, 23(5):1505–1518, 2015.

[6] M.R. Davoodi, N. Meskin, and K. Khorasani. Event-triggered multiobjective control and fault diagnosis: A unified framework. *IEEE Transactions on Industrial Informatics*, 13(1):298–311, 2016.

[7] D.M. Dawson, Z. Qu, and J.J. Carroll. Robust control of rigid-link electrically-driven robot manipulators. *International Journal of Control*, 56(5):991–1006, 1992.

[8] V.S. Dolk, D.P. Borgers, and W.P.M.H. Heemels. Output-based and decentralized dynamic event-triggered control with guaranteed $\mathcal{L}_p$-gain performance and Zeno-freeness. *IEEE Transactions on Automatic Control*, 62(1):34–49, 2017.

[9] M.C.F. Donkers and W.P.M.H. Heemels. Output-based event-triggered control with guaranteed $\mathcal{L}_\infty$-gain and improved and decentralized event-triggering. *IEEE Transactions on Automatic Control*, 57(6):1362–1376, 2012.

[10] R. Goebel, R.G. Sanfelice, and A.R. Teel. *Hybrid Dynamical Systems: Modeling, Stability, and Robustness.* Princeton University Press, 2012.

[11] T.M.P. Gommans, D. Antunes, M.C.F. Donkers, P. Tabuada, and W.P.M.H. Heemels. Self-triggered linear quadratic control. *Automatica*, 50(4):1279–1287, 2014.

[12] W.P.M.H. Heemels, K.H. Johansson, and P. Tabuada. An introduction to event-triggered and self-triggered control. *In Proceedings of the 51st IEEE Conference on Decision and Control, Maui, U.S.A.*, pages 3270–3285, 2012.

[13] W.P.M.H. Heemels, A.R. Teel, N. van de Wouw, and D. Nešić. Networked control systems with communication constraints: Tradeoffs between transmission intervals, delays and performance. *IEEE Transactions on Automatic Control*, 55(8):1781–1796, 2010.

[14] M. Kögel and R. Findeisen. On self-triggered reduced-attention control for constrained systems. *In Proceedings of the 53rd IEEE Conference on Decision and Control, Los Angeles, U.S.A.*, pages 2795–2801, 2014.

[15] F. Li, J. Fu, and D. Du. An improved event-triggered communication mechanism and $\mathcal{L}_\infty$ control co-design for network control systems. *Information Sciences*, 370-371:743762, 2016.

[16] X. Meng and T. Chen. Event detection and control co-design of sampled-data systems. *International Journal of Control*, 87(4):777–786, 2014.

[17] A. Molin and S. Hirche. Optimal event-triggered control under costly observations. *In Proceedings of the International Symposium on Mathematical Theory of Networks and Systems, Budapest, Hungary*, pages 2203–2208, 2010.

[18] D. Nešić and D.S. Laila. A note on input-to-state stabilization for nonlinear sampled-data systems. *IEEE Transactions on Automatic Control*, 47(7):1153–1158, 2002.

[19] D. Nešić, A.R. Teel, and D. Carnevale. Explicit computation of the sampling period in emulation of controllers for nonlinear sampled-data systems. *IEEE Transactions on Automatic Control*, 54(3):619–624, 2009.

[20] D. Nešić, A.R. Teel, G. Valmorbida, and L. Zaccarian. Finite-gain $\mathcal{L}_p$ stability for hybrid dynamical systems. *Automatica*, 49(8):2384–2396, 2013.

[21] R. Postoyan, P. Tabuada, D. Nešić, and A. Anta. A framework for the event-triggered stabilization of nonlinear systems. *IEEE Transactions on Automatic Control*, 60(4):982–996, 2015.

[22] C. Scherer, P. Gahinet, and M. Chilali. Multiobjective output-feedback control via LMI optimization. *IEEE Transactions on Automatic Control*, 42(7):896–911, 1997.

[23] P. Tabuada. Event-triggered real-time scheduling of stabilizing control tasks. *IEEE Transactions on Automatic Control*, 52(9):1680–1685, 2007.

[24] W. Wang, D. Nešić, and A.R. Teel. Input-to-state stability for a class of hybrid dynamical systems via averaging. *Mathematics of Control, Signals and Systems*, 23:223–256, 2012.

[25] X. Zhang and Q. Han. Event-based dynamic output feedback control for networked control systems. *In Proceedings of the American Control Conference, Washington, U.S.A.*, pages 3008–3013, 2013.